Light Metals 2011 *Edited by: Stephen J. Lindsay*
TMS (The Minerals, Metals & Materials Society), 2011

FEM ANALYSIS OF THE ANODE CONNECTION IN ALUMINIUM REDUCTION CELLS

Susann Beier[1], John J. J. Chen[1], Hugues Fortin[2] Mario Fafard[3 4]

[1]Light Metals Research Centre, University of Auckland, Auckland 1142, New Zealand
[2] Institut de recherche Hydro-Québec - LTE, 600 avenue de la Montagne Shawinigan, Canada, G9N 7N5
[3] NSERC/Alcoa Industrial Research Chair MACE
[4] Aluminium Research Centre - REGAL, Laval University, Sciences and Engineering Faculty, Québec, Canada, G1V 0A6

Keywords: anode connection, yoke bending, stub deterioration, stub diameter, stub replacement

Abstract

Achieving voltage savings over the anode assembly in an aluminium reduction cell, particularly at the anode connection, is a worthwhile approach within a wider programme of improvement in energy efficiency. Experiments carried out using operating cells are very difficult and expensive, however finite element method (FEM) simulations as used in this study are a cost efficient and accurate method to understand the behaviour of the anode connection, and to identify the constraints to voltage savings. This study investigates the impacts of stub deterioration and yoke stiffness on the anode connection and hence the performance of the anode assembly. An ideal stub diameter for the investigated configuration was found, and the increased voltage drops for various level of stub deterioration were identified. The results show that a yoke cross-bar with reduced height and hence reduced stiffness decreases the tensile stress developed in the carbon anode, which lowers the risk of anode cracks. A limit for stub service life is suggested, showing a potential saving of US$0.8m annually.

Introduction

The electrolysis process for aluminium production consumes the carbon anode block. After the anode is spent, the remaining 'butt' of the anode has to be replaced with a new anode. The anode assembly must be taken out of the cell, and carbon butt and cast iron thimble are stripped off the stubs. The steel yoke assembly is then inspected for damage, and re-used if the level of damage does not exceed specified smelter limits.

New carbon anode blocks are connected to the anode assembly using molten cast iron, which is poured into the spatial gap between the stubs and anode stub holes. The hot cast iron heats up the steel stubs, causing thermal expansion, giving a shrink fit of the cast iron onto the stubs. The cast iron shrinks when it solidifies, causing an air gap to develop at the cast iron - carbon interface. This air gap is critical to anode performance, as it increases the contact resistance of the anode connection. Research has shown that a voltage drop of 80 to 130 mV appears at the interface from stub to cast iron to carbon [1]. More than 90% of this is due to the cast iron to carbon interface [2]. The aggressive environment of high temperature and electro-chemical attack in the reduction cell can also cause deterioration and deformation of the anode assembly. The degree of stub deterioration and yoke bending are the major factors that determine the performance of the anode connection, influencing the stress, voltage and temperature distribution significantly.

The cast iron thimble formed on a new, non-deteriorated stub is relatively thin, and hence the shrinkage of cast iron is small, giving a narrow air gap at the cast iron - carbon interface. The small air gap results in rapid tightening of the connection when the anode heats in the cell. This saves early-cycle voltage losses, but also causes higher stresses in the carbon anode and greater risk of harmful vertical anode cracking.

Conversely, when deteriorated stubs are re-used, more cast iron is required at the connection to fill the anode stub hole, giving increased cast iron shrinkage and hence a larger air gap. This air gap creates high early-cycle voltage losses, as the air gap closes later in the anode cycle. The stress in the carbon anode is significantly lower however, and the risk of anode cracking is decreased.

The high temperature environment in the aluminium reduction cell causes significant thermal expansion in the yoke. For a three-stub assembly geometry as studied in this work, the yoke expansion causes a bending moment and hence radial pressure increase at the outer stubs. This can have an significant impact on the stress development in the carbon anode block and needs to be further investigated [3].

Research Aim

The cast iron - carbon interface at the anode connection has a thermo-electro-mechanical interrelated behaviour which is strongly influenced by stub deterioration and yoke bending. The investigation of this behaviour by *in situ* plant measurements during cell operation is a very difficult and expensive approach. This study focuses on computational FEM simulation of an anode assembly, presenting a cost efficient and qualitative approach.
The following key research questions were developed, which form the main objectives of this study:

- What is the ideal ratio of stub diameter to cast iron thickness for the investigated configuration, to prevent anode cracks and give maximum voltage savings at the anode connection?
- How significant is the impact of stub deterioration on the anode connection and hence on the anode assembly performance?
- Does yoke bending increase tensile stresses in the carbon anode, causing increased risk of vertical anode cracks?
- How long is the ideal stub service life before replacement for greatest economic benefit?

Previous Work

This research is based on the work by Richard et al. [4] who developed the first weakly thermo-electrical-mechanical (TEM) coupled FEM model, which contributed to the development of a constitutive cast iron - carbon resistance model [5]. Goulet [6] further improved the TEM coupling, and implemented the FEM solver FESh++ for Hall-Héroult Aluminium reduction cells.
This work was progressed by Fortin et al. [7] and Richard et al. [8]. Fortin investigated the impact of stub deterioration by varying the stub shape, showing that the outer stub holes of a three stub anode assembly have more impact on the anode performance than the middle stub. Richard simulated and compared anode assemblies with a different number of cast iron flutes, showing that the benefit of an increased number of flutes is limited.
The anode assembly model presented and studied in this work is based on the simulation code used by Fortin and Richard, provided by the Aluminium Research Centre - REGAL from Laval University. The anode assembly code was enhanced in APDL (ANSYS Parametric Design Language), and the simulation was solved with FESh++, the FEM solver for Hall-Héroult aluminium reduction cells developed by REGAL [6].

FEM Model

The FEM model of an anode assembly consists of an aluminium rod, a steel yoke, three aligned steel stubs with cast iron thimbles, and the carbon anode block as shown in Figure 1. The models dimensions and design are widely used in industry and are based on Fortin et al. [9].

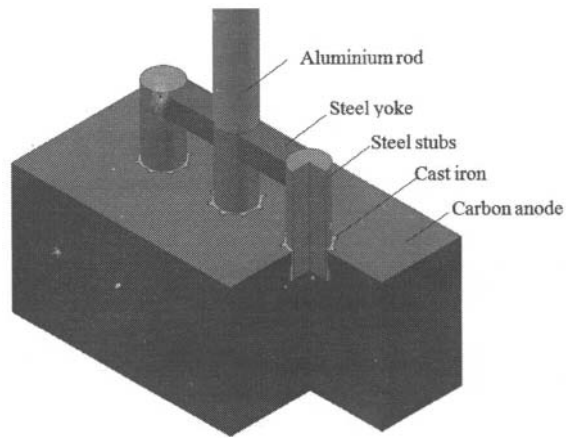

Figure 1: Generated FEM anode assembly model

The main model dimensions are: anode width 700 mm, anode length 1500 mm, anode height 650 mm, stub centre distance 500 mm, stub diameter 190-160 mm, stub hole diameter 209 mm, stub hole depth 130 mm, yoke cross-bar width 120 mm, yoke cross-bar heights 93 and 100mm. Various boundary conditions were applied to represent the operational conditions in an aluminium reduction cell:

- Immersion height of the anode into the bath of 400 mm.
- Hot gas immersion from the bath of 150 mm height.
- Height of cover and crust layer of 350 mm.
- The bottom face of the anode block is defined as zero voltage.
- The applied current density is dependent on rod diameter and assumed a total line current of 330 kA and 40 anodes per cell.
- Gravity and the buoyancy force are applied to the anode block.

- Several convective and radiative heat fluxes were applied over the anode assembly taking into account the hot air, crust, gas and bath conditions as well as anode position in the cell [6, 9].

Air Gap Prediction and Plant Measurement Comparison

The air gap developed at the cast iron - carbon interface depends on various factors which are not yet fully understood. Richard [8] proposed a comprehensive method to predict the air gap. This validated simplified analytical method is given in Equations (1) to (3).

$$s_{gap} = \gamma_S + (t - \gamma_S) \cdot \alpha_{CI} \cdot (T_{CI} - T_0) \quad (1)$$

$$\gamma_S = r_S \cdot \alpha_S \cdot (T_S - T_0) \quad (2)$$

$$t = \frac{d_{sh}}{2} - r_S \quad (3)$$

Where:

s_{gap} = Air gap size at T_0, mm
γ_S = Change in radius of the steel stub, mm
t = Stub hole gap, mm
α_{CI} = Thermal expansion coefficient of cast iron, $\frac{1}{K}$
T_{CI} = Temperature of cast iron, °C
T_0 = Ambient temperature, °C
r_S = Stub radius, mm
α_S = Thermal expansion coefficient of steel, $\frac{1}{K}$
T_S = Temperature of steel stub, °C
d_{sh} = Stub hole diameter, mm

The initial air gap size s_{gap} is calculated for the ambient temperature T_0 as shown in Equation (1). The cast iron solidification temperature T_{CI} is assumed to be 1200°C with the ambient temperature T_0 of 20°C and the thermal expansion coefficient of cast iron α_{CI} of $9 \cdot 10^{-6} \frac{1}{K}$. The change in radius of the steel stub is described by γ_S in Equation (2). It is determined by the ambient temperature T_0, the effective stub temperature when cast iron solidifies T_S at 200°C [10], the stub radius r_S and the thermal expansion coefficient of steel α_S of $1.5 \cdot 10^{-6} \frac{1}{K}$. The change in spatial gap, t, between stub hole and stub is given by Equation (3).
Limitations of this method were found for cast iron configurations with flutes, where the prediction method results in a too large air gap for the large cast iron thickness at the flutes. Cast iron shrinkage appears non-linear to its thickness, and Richard's method is only valid for a certain range of cast iron thickness.
Simulations with various air gap sizes were developed and solved, and compared to *in situ* measurements from industry. It was found that a reduction of 13.5% of the initial calculated air gap, as given by Equation (4), best matched actual measured voltage drops from industry.

$$s_{gap\ flutes} = s_{gap} \cdot 0.865 \quad (4)$$

Where:

$s_{gap\ flutes}$ = Air gap size at cast iron flutes, mm

The air gap used in the FEM model at the cast iron body was calculated by Richard's method, and the air gap at the cast iron flutes was reduced as given by Equation (4). This approach gave the best agreement with the temperature and voltage measurements of 10 anode assemblies taken in Smelter 'A'. Temperature measurements were taken at 14 points over the anode assembly, with voltage drops taken at 9 different measurement points. All predicted model results fell within the range of both the temperature and voltage measurements. For reasons of confidentiality no further information can be published on the plant measurements.

Model Application

Two case studies were performed: firstly, the base model was modified by using different stub diameters of 190, 180, 170 and 160 mm with a constant stub hole diameter of 209 mm, representing different stages of stub deterioration. The different stub configuration models were solved and compared with respect to temperature, stress, voltage and current distributions. These models allow conclusions to be drawn on the influence of re-usage of deteriorated stubs.
Secondly, each of the stub configuration models were solved using a reduced yoke cross-bar height of 93 instead of 100mm. The reduced height results in a decreased second moment of area, and reducing flexural stiffness by 20% as shown by Equations (5) and (7).

$$J_x = \frac{w \cdot h^3}{12} \quad (5)$$

$$J_{x\ 1} = \frac{120 \cdot 100^3}{12} = 10,000,000 \quad (6)$$

$$J_{x\ 2} = \frac{120 \cdot 93^3}{12} = 8,043,570 \quad (7)$$

Where:

J_x = Second moment of area, mm^4
w = Width of the sectional area, mm
h = Height of the sectional area, mm

The reduced flexural stiffness results in greater bending of the yoke, causing increased radial pressure at the outer stubs and stub holes. The comparison of various stub configuration models with 93 and 100mm yoke height clarified the effect of yoke stiffness on the anode connection. These predicted model results allowed development of a cost analysis, where voltage drop increase due to stub deterioration, anode cracking, material and replacement costs are taken into account. Potential voltage savings at the anode connection are identified, and suggestions for an ideal stub service life are made.

Results and Discussion

Stub Deterioration

The simulation of anode assemblies with various stub configurations showed that the normal stress at the interface is significantly lower for smaller stub sizes when the cast iron thickness and hence the air gap is increased. The increased air gap however causes a higher contact resistance and higher voltage drop as shown in Figure 2. A voltage drop increase of 68% was found at the anode connection for a stub diameter reduction of 16%.

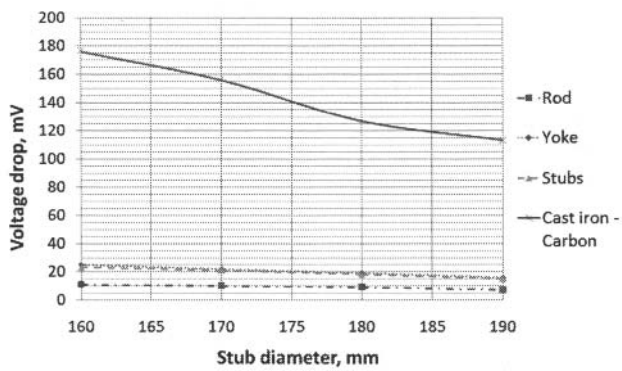

Figure 2: Voltage prediction for stub configurations

The larger air gap causes low contact pressure, which increases the electrical resistance R_E. This leads to high local current density over the actual contact surface. The high current density I increases the ohmic heat Q generation as given by Equation (8).

$$Q = I^2 \cdot R_E \tag{8}$$

The cast iron temperature increased by 13% with stub deterioration by 16%. This temperature is conducted to the cooler upper parts of the anode assembly, and the connection, stubs, yoke and rod all show a slightly increased temperature as shown in Figure 3. The higher temperature of the materials leads to slightly higher electrical resistance causing a further increased voltage drop as shown in Figure 2.

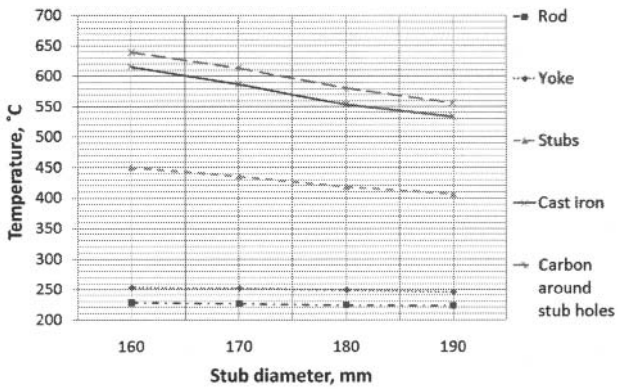

Figure 3: Temperature prediction for stub configurations

The highest stresses in the carbon anode was found at the stub hole flutes. The local stresses were very high, and decrease rapidly from the carbon top to the bottom. For a stub diameter of 190mm with a cast iron thimble of 9.5 mm thickness, the local stress predicted is very high and likely to exceed the carbon anode stress limits. The local stresses decreased strongly by 33% with a 16% decrease in stub diameter as shown in Figure 4.

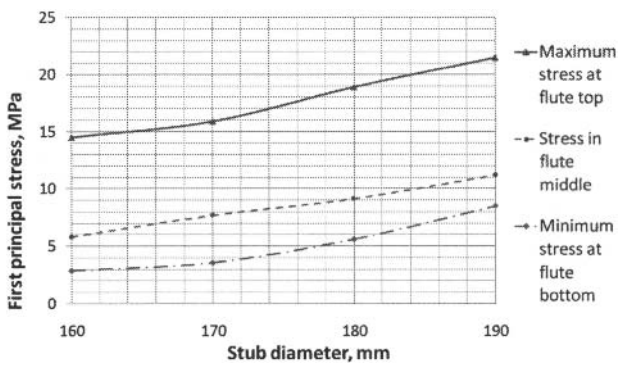

Figure 4: Predicted tensile stress in stub hole flutes

Yoke Stiffness

Simulation models were developed with various stub diameters and yoke cross-bar height reduced from 100 to 93mm, giving 20% reduction in yoke stiffness and hence increased yoke bending. The simulation results for the various stub diameters from 190 to 160mm were compared, and no significant differences in voltage or temperature distribution were found with reduced yoke height. The tensile stress strongly reduced in average in the carbon flutes however, by around 22% as shown in Figure 5. It was seen that the increased radial pressure due to increased yoke bending reduced the tensile stress at the top of the stub hole, and increased the compressive stress at the bottom of the stub hole. The stress limit of carbon anode is significantly higher in compression than in tension [11]. This results in a lower risk of anode cracks formation for the 180mm diameter stub configuration. It can be concluded that increased yoke bending and the radial pressure increase has a positive impact on the stress development in the anode carbon block.

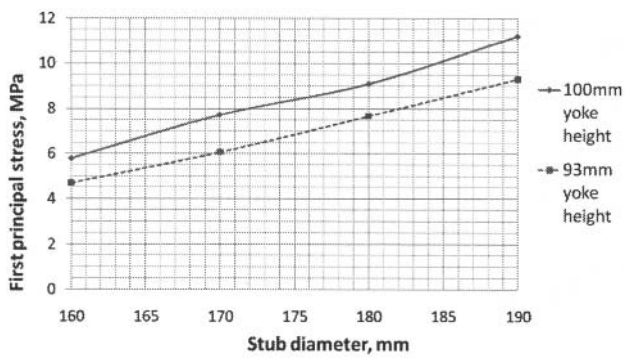

Figure 5: Predicted tensile stress in the carbon anode flutes

Cost Analysis

The lowest anode voltage drop found without exceeding carbon stress limits was found for the configuration with 180mm stub diameter and 93mm yoke height. This is taken as the initial configuration in the cost analysis, which assumes a operation at 330kA with US$0.044 costs per kWh and uses various assumption based on smelter cost statistics as discussed by Beier [12].

The simulation results showed that the voltage drop increases with decreasing stub diameter, giving additional annual operational costs as shown in Figure 6 as solid line.

Additional material and operational costs are incurred due to earlier stub replacement. The material cost of a 180 mm steel stub was assumed to be US$47. With an average stub life cycle of 15 anode cycles and a replacement cost of US$51.3, additional annual costs due to earlier stub replacement accrue as a function of the specified minimum stub diameter before replacement.

In addition to these costs, the risk of anode cracks was also taken into account. The maximum stress developed in the anode block was found from the simulation results, while a stress limit for the carbon anode was assumed. The local stress was used to find a percentage increase in voltage drop, assuming the maximum voltage drop occurs in the case of an anode breakage when the maximum stress limitation is reached. The maximum voltage drop due to an anode breakage was simulated, and the voltage drop for lower local stress values was found assuming a linear relationship due to partial anode cracking. These additional annual costs were added to the calculated cost due to stub replacement, and are also shown in Figure 6 as dashed line.

The cost due to increased voltage drop outweighed the cost caused by stub replacement and risk of anode cracking below a stub size of 139mm, equivalent to 41mm or 28% deterioration in stub diameter.

A common smelter procedure found in an industry survey is to replace a deteriorated stub after approximately 28% diameter reduction to 130mm [13, 14]. This study suggests replacement after approximately 23% reduction to 139 mm, giving US$800,000 annual saving in voltage drop for a smelter with 264 pots operating.

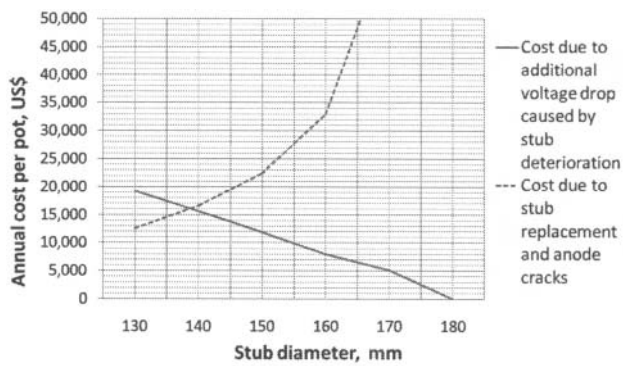

Figure 6: Comparison of annual cost per pot by voltage drop against cost by stub replacement and anode cracks

Conclusions

In this study a FEM model of the anode assembly was used with an adjustment of the air gap prediction for a fluted cast iron connection. The adjusted simulation model results compared well with *in situ* voltage and temperature measurements from industry. Various stub and yoke configurations were subsequently investigated regarding voltage drop, temperature, current and stress distributions.

It was found that reduced yoke stiffness significantly decreased the tensile stresses in the carbon anode. For the anode assembly design investigated, the configuration with 180 mm stub diameter and 93 mm yoke crossbar height gave the best compromise between low voltage drop and stress development below the critical carbon anode tensile stress limit.

A cost analysis based on the simulation results showed that the cost due to increased voltage drop caused by stub deterioration is very high. A common smelter practise is to replace stubs after approximately 28% deterioration, while this analysis however showed that earlier replacement after only 23% stub deterioration could lead to significant annual savings due to reduced voltage drop.

Acknowledgement

I would like to thank Olivier Trempe and the Aluminium Research Centre - REGAL, Laval University, Québec City, Stew Woodward (Rio Tinto Alcan, NZAS), Barry Sadler (Net Carbon Consulting Pty Ltd) and Michael Gasse (Alcoa, Deschambault) as well as Pascal Lavoie and the rest of the Light Metals Research Centre team for your collaboration, advice and support.

References

[1] W. T. Choate and J. A. S. Green, "U.S. Energy Requirements for Aluminium Production," 2003.

[2] J. Wilkening and S. Cote, "Problems of the Stub-Anode Connection," *TMS Light Metals*, pp. 865–873, 2007.

[3] N. A. Ambenne, "Vertical Anode Cracking - The VALCO Experience," *TMS Light Metals*, vol. 1, pp. 577–583, 1997.

[4] D. Richard, M. Fafard, R. Lacroix, P. Clery, and Y. Maltais, "Aluminum Reduction Cell Anode Stub Hole Design using weakly coupled Thermo-Electro-Mechanical Finite Element Models," *Finite elements in analysis and design*, vol. 37, pp. 287–304, 2001.

[5] D. Richard, M. Fafard, R. Lacroix, P. Clery, and Y. Maltais, "Carbon to Cast Iron Electrical Contact Resistance Constitutive Model for Finitie Element Analysis," *Journal of Materials Processing Technology*, vol. 1, pp. 119–131, 2003.

[6] P. Goulet, *Modélisation du comportement thermo-électro-mécanique des interfaces de contact d'une cuve de Hall-Héroult.* PhD thesis, Laval University, Québec, Canada, 2004.

[7] H. Fortin, M. Fafard, N. Kandev, and P. Goulet, "FEM Analysis of Voltage drop in the Anode Connector Assembly," *TMS Light Metals*, vol. 1, p. 6, 2009.

[8] D. Richard, P. Goulet, O. Trempe, M. Dupuis, and M. Farad, "Challenges in Stub Hole Optimisation of Cast Iron rodded Anodes," *TMS Light Metals*, vol. 1, p. 6, 2009.

[9] H. Fortin, "Modélisation du comportement thermo-électro-mécanique de l'anode de carbone utilisée dans la production primaire de l'aluminium ," Master's thesis, Laval Univeristy, Québec, Canada, 2010.

[10] O. Trempe, D. Larouche, D. Ziegler, M. Guillot, and M. Fafard, "Real time temperature distribution during sealing process and room temperature air gap measurements of a Hall-Héroult cell anode," *TMS Light Metals*, 2011. to appear.

[11] O. E. Frosta, T. Foosnaes, H. A. Øye, and H. Linga, "Modelling of Anode Thermal Cracking Behaviour," *TMS Light Metals*, vol. 1, pp. 923–927, 2008.

[12] S. Beier, "A Study of an Anode Assembly with Focus on the Anode Connection used in Aluminium Reduction Cells ," Master's thesis, Auckland Univeristy, July 2010.

[13] S. Woodward, "Personal communication," *from Rio Tinto Alcan, New Zealand Aluminium Smelters (NZAS)*, 2010.

[14] M. Gasse, "Personal communication," *from Aluminerie Deschambault Québec, Alcoa, through the Aluminium Research Centre - REGAL, Québec, Canada*, 2010.